Crystal structure of a high-pressure/high-temperature phase of alumina by *in situ* X-ray diffraction

JUNG-FU LIN[1]*, OLGA DEGTYAREVA[1], CHARLES T. PREWITT[2], PRZEMYSLAW DERA[1], NAGAYOSHI SATA[3], EUGENE GREGORYANZ[1], HO-KWANG MAO[1] AND RUSSELL J. HEMLEY[1]

[1]Geophysical Laboratory, Carnegie Institution of Washington, Washington DC 20015, USA

[2]Department of Geosciences, University of Arizona, Tucson, Arizona 85721, USA

[3]Institute for Frontier Research on Earth Evolution, Japan Marine Science and Technology Center, Kanagawa 237-0061, Japan

*e-mail: j.lin@gl.ciw.edu

Published online: 16 May 2004; doi:10.1038/nmat1121

Alumina (α-Al_2O_3) has been widely used as a pressure calibrant in static high-pressure experiments[1–4] and as a window material in dynamic shock-wave experiments[5–14]; it is also a model material in ceramic science. So understanding its high-pressure stability and physical properties is crucial for interpreting such experimental data, and for testing theoretical calculations[15–21]. Here we report an *in situ* X-ray diffraction study of alumina (doped with Cr^{3+}) up to 136 GPa and 2,350 K. We observe a phase transformation that occurs above 96 GPa and at high temperatures. Rietveld full-profile refinements show that the high-pressure phase has the Rh_2O_3 (II) (*Pbcn*) structure, consistent with theoretical predictions[22]. This phase is structurally related to corundum, but the AlO_6 polyhedra are highly distorted, with the interatomic bond lengths ranging from 1.690 to 1.847 Å at 113 GPa. Ruby luminescence spectra from Cr^{3+} impurities within the quenched samples under ambient conditions show significant red shifts and broadening, consistent with the different local environments of chromium atoms in the high-pressure structure inferred from diffraction. Our results suggest that the ruby pressure scale needs to be re-examined in the high-pressure phase, and that shock-wave experiments using sapphire windows need to be re-evaluated.

The pressure-induced red shift of the Cr^{3+} luminescence wavelength of ruby (Cr^{3+} doped α-Al_2O_3) has been calibrated with Au up to180 GPa, and is commonly used as a secondary pressure standard in high-pressure diamond-anvil cell (DAC) research[1–4]. Because it is often desirable to maintain as high a pressure as possible at the interface of the sample and window materials in shock-wave experiments, corundum, a high-rigidity, transparent material, is commonly used as a window material to transmit light for velocity measurements and temperature determination[5–14].

Theoretical calculations have predicted that corundum (space group $R\bar{3}c$) transforms to the Rh_2O_3 (II) structure (space group *Pbcn*) and then to the orthorhombic perovskite structure (space group *Pbnm*)[15–21], although the predicted transition pressure varies because of different models used. There have been considerable theoretical efforts to understand the structural, optical, electronic and elastic properties of the high-pressure polymorphs of alumina[15–21], but detailed experimental data are still lacking[3,4]. One static X-ray diffraction study on corundum indicated that a phase transformation occurred at ~100 GPa and ~1,000 K and that the high-pressure phase had the orthorhombic structure (possibly in the Rh_2O_3 (II) structure[22]); however, the diffraction patterns contained unexplained peaks and the high-pressure phase was not confirmed by structure refinement[4]. X-ray diffraction results at pressures up to 175 GPa at ambient temperature can be interpreted with the corundum structure[3]. Therefore, it is evident that high temperatures are required for the transition to take place[4,18]. Recent shock-wave experiments on corundum showed that two transitions occurred at 79 GPa and 250 GPa (refs 13, 14), consistent with the theoretical calculations[15–21]. A structural phase transformation in corundum under high pressures would change its optical properties, and hence affect the calibration of the ruby pressure scale at ultrahigh pressures, as well as affecting the interpretation of the shock-wave experiments carried out with corundum windows for velocity and temperature measurements[1,2,5–14]. To understand the crystal structure and crystal chemistry of the high-pressure phase and the effects of the phase transformation on static and dynamic high-pressure experiments, we studied α-Al_2O_3 with *in-situ* X-ray diffraction in a laser-heated DAC up to approximately 136 GPa and 2,350 K.

Polycrystalline alumina (α-Al_2O_3, 99.99% pure) was obtained from Johnson Matthey. The ruby luminescence peaks were strong enough to be detected because of the presence of a minute amount of Cr^{3+} in the sample. The sample (with a grain size of ~1 μm) was well mixed with 2–8 wt% of Pt (which served as an absorber of the laser light and an internal pressure standard[23]) in a moulded corundum mortar (Diamonite mortar from Fisher Scientific). Angle-dispersive X-ray diffraction under ambient conditions showed that the sample had the corundum structure ($R\bar{3}c$), and that Pt was in the face-centred cubic ($Fm\bar{3}m$) structure. A rhenium gasket was pre-indented to a thickness of 35 μm between bevelled diamonds with an inner culet of 150 μm and an

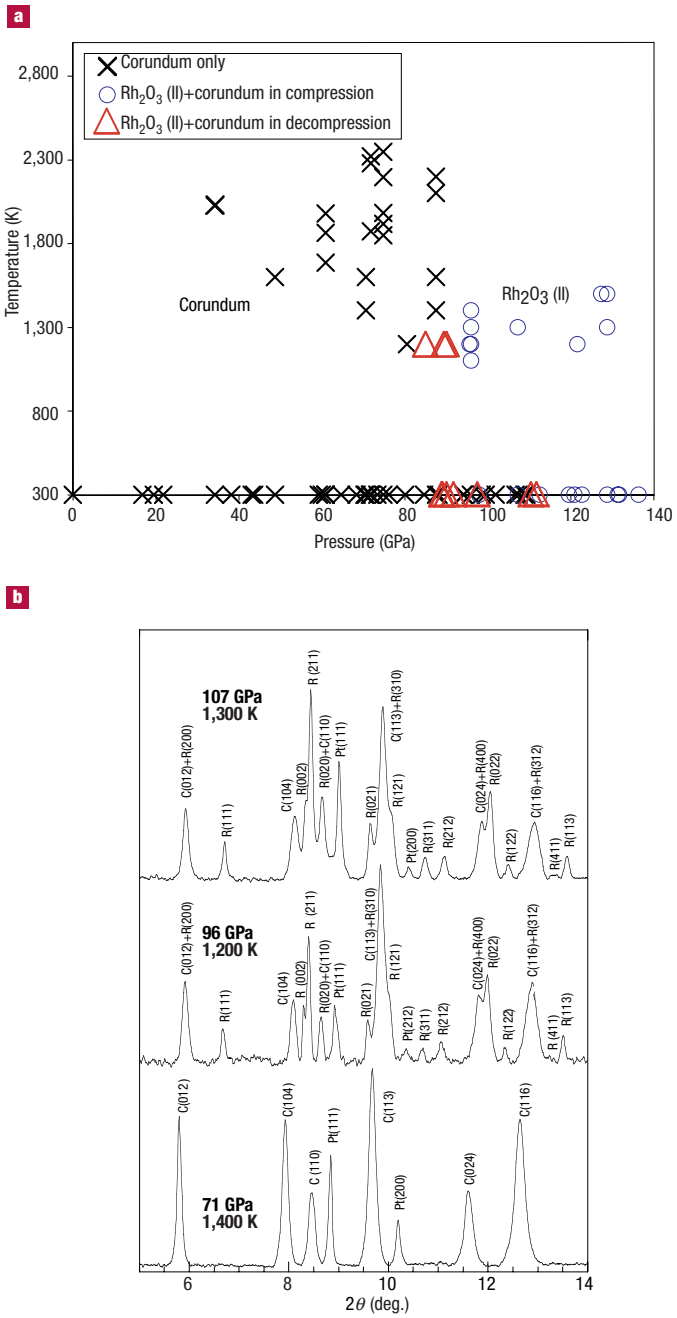

Figure 1 ***In situ*** **X-ray diffraction study of Al_2O_3 under high pressures and high temperatures. a**, Phases observed in Al_2O_3 under high pressures and high temperatures. Black crosses, Al_2O_3 in the corundum structure; blue open circles, Al_2O_3 in the Rh_2O_3 (II) and corundum structure observed during compression; red open triangles, Al_2O_3 in the Rh_2O_3 (II) and corundum structure observed during decompression. All samples were first compressed to a specific pressure at 300 K and then heated to high temperatures, where X-ray diffraction patterns were taken if possible. After each heating cycle, the sample was compressed to higher pressure at 300 K and then heated again. A phase transformation from corundum to Rh_2O_3 (II) structure is observed to occur above 96 GPa and at high temperatures in the compression process. The high-pressure phase can still be seen as low as 85 GPa on decompression, indicating the sluggish character of the phase transformation. As the transition only occurred at high temperatures, the symbols representing two phases at 300 K only indicate observation of the two phases after laser heating. **b**, Representative angle-dispersive X-ray diffraction patterns of Al_2O_3 at high pressures and high temperatures. A monochromatic beam (wavelength 0.3311 Å) was used as the X-ray source, and the diffracted X-rays were collected by a CCD. The corundum structure was observed at 71 GPa and 1,400 K. A phase transformation occurred at 96 GPa and 1,200 K (the surrounding unheated sample remained in the corundum phase). The peak intensities of the Rh_2O_3 (II) phase increased with increasing pressure, while the peak intensities of the corundum phase decreased (that is, R(111) and R(211) became relatively stronger than C(104) as pressure increased), indicating the two-phase character of the sample as this has also been observed in a separate sample (see Supplementary Fig. 2). Peak identifications are: C, Al_2O_3 in the corundum structure; R, Al_2O_3 in the Rh_2O_3 (II) structure; Pt, platinum as internal pressure calibrant.

outer culet of 300 μm, and a hole of 250 μm diameter was drilled in it. The hole was filled with an amorphous boron and epoxy mixture (4:1 by weight) and compressed[24]. Subsequently, another hole of 100 μm was drilled and used as the sample chamber. A sandwiched sample configuration, using dried NaCl or Al_2O_3 as the thermal insulator and pressure medium, was used in this study. The amorphous boron provides higher strength to create a deeper sample chamber, giving stronger X-ray diffraction from a thicker sample and better laser-heating spots because of thicker thermal insulating layers. Use of the light and amorphous boron avoids unwanted X-ray diffraction peaks from the gasket, making it possible to refine the crystal structure of the high-pressure phase with powder X-ray diffraction data under ultrahigh pressures and temperatures[24].

In situ X-ray diffraction experiments in a laser-heated DAC were conducted at the BL10XU sector of SPring-8, Japan, and the HPCAT and GSECARS sectors of the Advanced Photon Source, Argonne National Laboratory[25,26]. A double-sided laser heating system (Nd:YAG or Nd:YLF laser) was used to heat the sample from both sides[25,26], and grey-body temperatures were determined by fitting the thermal radiation spectrum between 670 and 830 nm to the Planck radiation function. The diameter of the laser beam at the sample position was about 25 μm. Focused monochromatic beams (wavelength 0.4113 Å at BL10-XU, 0.3698 Å at HPCAT, or 0.3311 Å at GSECARS) with beam sizes of approximately 10 μm diameter were used as the X-ray source for angle-dispersive X-ray diffraction experiments. The diffracted X-rays were collected with an image plate (Rigaku R-Axis (IV) or MAR345) or by a CCD (Bruker-2k). Pressures were calculated from the equation of state of Pt (ref. 23). The diffraction patterns were processed with FIT2D[27], PeakFit 4.0, and General Structure Analysis System (GSAS) programs[28].

In situ high-pressure/high-temperature X-ray diffraction patterns and phases observed are shown in Fig. 1a and b. The corundum structure was observed up to 109 GPa and 300 K without laser heating (Fig. 1a). While laser-heated, a phase transformation was observed to occur above 96 GPa and at high temperatures, showing that temperature is required for the transformation to occur (Fig. 1b). As pressure and temperature increased above the transition, the peak intensities of the high-pressure phase increased relative to the corundum peaks (Fig. 1b; see Supplementary Information for details). But the high-pressure phase coexisted with the corundum phase up to 136 GPa even after laser heating, suggesting that some corundum in contact with diamond was not totally transformed to the high-pressure phase and a large kinetic barrier may exist in the phase transformation. The difference in relative intensities of the two phases in two separate samples indicates the two-phase character of the samples (Fig. 1b; Supplementary Fig. 2). Moreover, a series of X-ray diffraction patterns were collected from the laser-heated area to the surrounding unheated area at ~100 GPa. The X-ray intensities of the high-pressure phase were much stronger in the laser-heated area while the unheated sample remained in the corundum phase, indicating that the sample consists of two phases.

Table 1 Refined structural parameters of the high-pressure phase of alumina at 113 GPa and 300 K. Refinement was performed using Rietveld full-profile refinement in the GSAS program[28]. Numbers in parentheses are the standard deviations or the multiplicity of the interatomic bonds.

	Parameter	Corundum	Rh_2O_3 (II)	Perovskite	
Structure					
	Space group	$R\bar{3}c$	*Pbcn*	*Pbnm*	
	a (Å)	4.374 (2)	6.393 (1)	4.362 (1)	
	b (Å)	4.374 (2)	4.362 (1)	4.544 (1)	
	c (Å)	11.829 (7)	4.543 (1)	6.395 (1)	
	Al1	(0,0,0.350)	(0.114,0.758,0.028)	(0.509,0.545,0.250)	
	Al2			(0.5,0,0.5)	
	O1	(0.319,0,0.250)	(0.849,0.619,0.120)	(0.111,0.370,0.250)	
	O2		(0,0.046,0.250)	(0.178,0.160,0.581)	
Bond lengths					
				Al1–O	Al2–O
	Al–O (Å)	1.688 (×3)	1.690 (×1)	1.664 (×2)	1.567 (×1)
		1.826 (×3)	1.727 (×1)	1.772 (×2)	1.606 (×2)
			1.731 (×1)	1.805 (×2)	1.910 (×1)
			1.768 (×1)		2.197 (×2)
			1.792 (×1)		2.328 (×2)
			1.847 (×1)		2.744 (×1)
	<Al–O> (Å)	1.757	1.759	1.747	2.054
	Al–Al (Å)	2.356 (×1)	2.489 (×1)	2.613 (×2)	
		2.556 (×3)	2.576 (×1)	2.680 (×2)	
		2.982 (×3)	2.694 (×1)	2.743 (×2)	
			2.789 (×2)	2.948 (×2)	
			2.862 (×2)		
			2.916 (×1)		
	<Al–Al> (Å)	2.709	2.747	2.747	

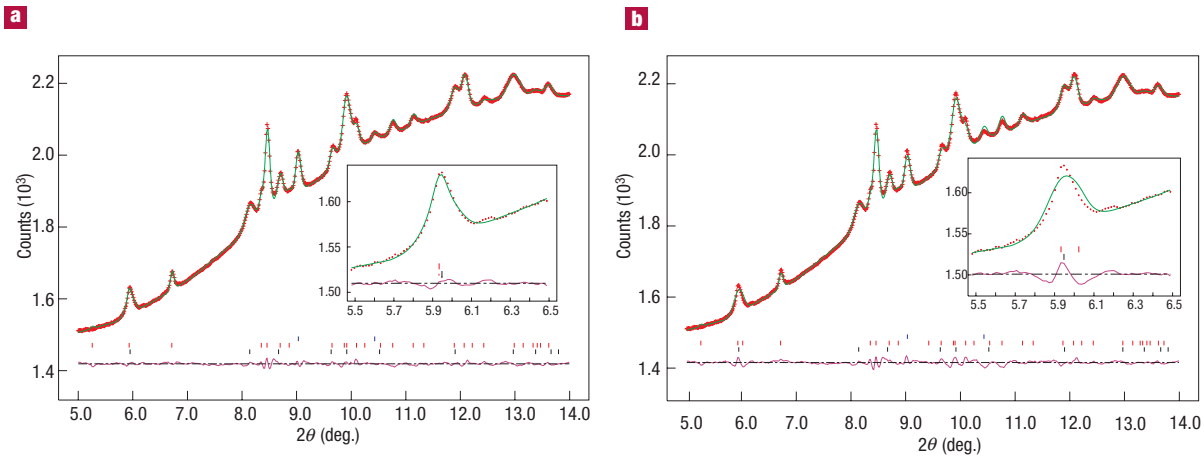

Figure 2 Typical Rietveld full-profile refinement, performed using the GSAS program[28], of the X-ray diffraction pattern collected at 113 GPa and 300 K after laser heating. **a**, Full-profile refinement using the Rh_2O_3 (II) structural model with corundum and Pt. As revealed from Rietveld refinement, the sample contained 60% Rh_2O_3 (II) phase, 39% corundum phase, and 1% Pt internal standard. Inset represents fits in the Rh_2O_3 (II) structure model in the region of $2\theta \approx 6°$. **b**, Full-profile refinement using the orthorhombic perovskite structural model with corundum and Pt. Inset (same parameters and units on *x* and *y* axes as main plot) represents misfits in the perovskite structural model in the region of $2\theta \approx 6°$. Whereas the diffraction near $2\theta \approx 6°$ shows one single peak, there should be two diffraction peaks (002 and 110) in the perovskite model. Red crosses, green solid line, and purple solid line represent experimental, modelled, and difference spectra, respectively. Blue ticks, Pt; black ticks, Al_2O_3 in corundum structure; red ticks, Al_2O_3 in the Rh_2O_3 (II) structure or the orthorhombic perovskite structure.

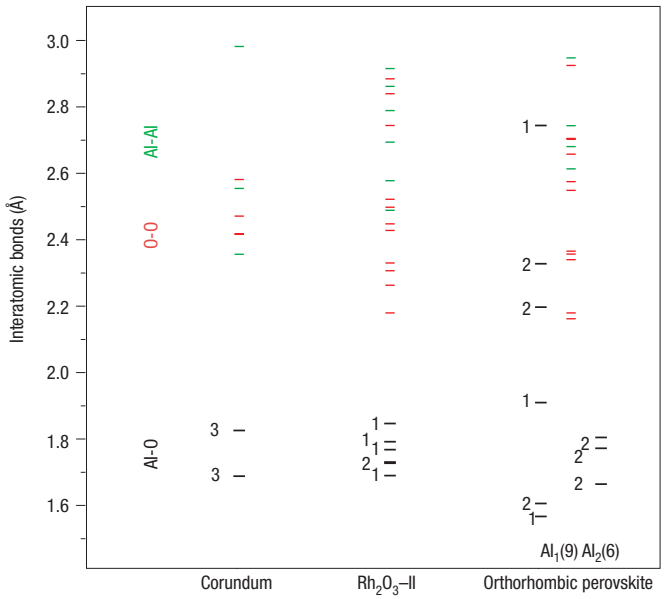

Figure 3 Interatomic bond lengths (Al–Al, Al–O and O–O bonds) of Al_2O_3 at 113 GPa and 300 K in the corundum, Rh_2O_3 (II), and orthorhombic perovskite structure model (Table 1). The AlO_6 octahedra are quite regular in the corundum structure, whereas they are rather deformed in the Rh_2O_3 (II) structure, with Al–O bond lengths ranging from 1.690 to 1.847 Å. The nine- and six-coordinated Al are also highly distorted in the orthorhombic perovskite structure. The averaged Al–O bond lengths across the phase transition increase slightly from 1.757 to 1.759 Å in the Rh_2O_3 (II) model, while they decrease from 1.757 to 1.747 Å in the perovskite model. Numbers near horizontal bars represent multiplicity of the bonds. Green bars, Al–Al bonds; red bars, O–O bonds; black bars, Al–O bonds.

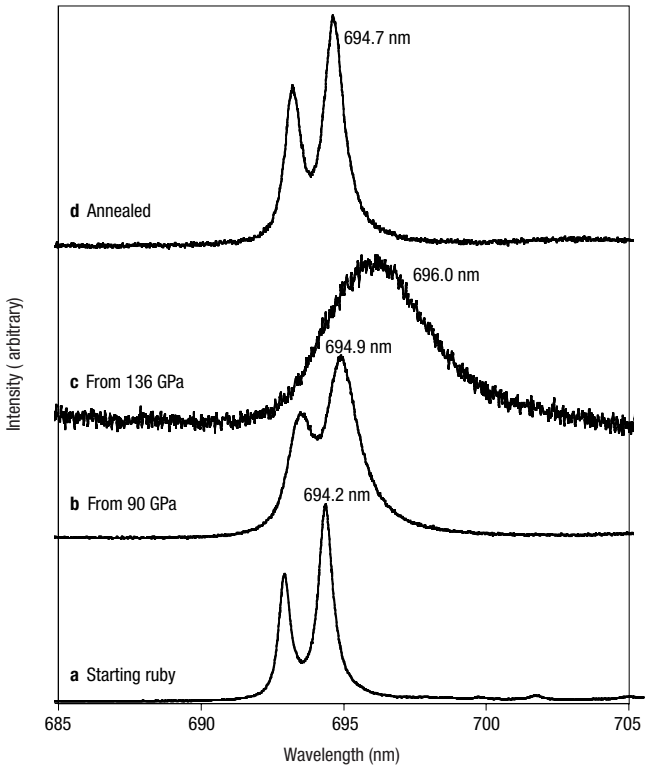

Figure 4 Ruby luminescence peaks measured under ambient conditions. a, Starting α-Al_2O_3 (luminescence band R_1 at 694.2 nm). **b**, Quenched from 90 GPa after laser heating (sample was in the corundum structure under high pressures). The luminescence R bands of the sample show slight red shifts (R_1=694.9 nm). **c**, Quenched from 136 GPa after laser heating (sample was in the Rh_2O_3 (II) and corundum structure). The luminescence R bands of the sample show significant broadening and a strong red shift (R_1=696.0 nm). **d**, Laser annealing at ~1,200 K and room pressure on the sample quenched from 136 GPa (R_1=694.7 nm). The ruby luminescence spectrum is similar to that of the starting material.

At first sight, the diffraction pattern of the high-pressure phase can only be explained either by the Rh_2O_3 (II) structure or the orthorhombic perovskite structure (Fig. 2, Tables 1, 2). Rietveld full-profile refinement and detailed analyses of the interatomic bond lengths show that the high-pressure phase is in the Rh_2O_3 (II)-*Pbcn* structure. Although the peak positions are all similar in the Rh_2O_3 (II) and the orthorhombic perovskite structure model, the calculated diffraction profile for the perovskite structure model shows some significant misfits with the data (Fig. 2). With a volume decrease of 3.1% across the phase transformation in both models, the averaged Al–O interatomic bond length increases slightly in the AlO_6 octahedra of the Rh_2O_3 (II) model whereas the averaged bond length decreases by 0.01 Å in the perovskite model (Figs 2, 3; Table 1). As the Al atoms are in nine- and six-coordinated sites in the perovskite model, a decrease in Al–O bond length would suggest a large volume change across the phase transformation, making the perovskite model thermodynamically unstable. The average Al–Al bond length increases by 1.4% across the corundum–Rh_2O_3 (II) phase transformation. The AlO_6 octahedra are quite regular in the corundum structure, whereas the AlO_6 octahedra are rather deformed in the Rh_2O_3 (II) model, with Al–O bond lengths ranging from 1.690 to 1.847 Å (Fig. 3). The Al–O, O–O and Al–Al interatomic bond lengths in the Rh_2O_3 (II) model are consistent with those from theoretical calculations (Table 1)[19]. The *c*/*a* ratio of corundum decreases with increasing pressure at a rate of 0.0002 GPa^{-1}, which would eventually lead to the distortion of the AlO_6 octahedra and the bending of the Al–O–Al bond angles.

The noticeable feature of the phase transformation from corundum to Rh_2O_3 (II) is the lowering of symmetry and differentiation of the bond lengths, suggesting further *d*-level electronic splitting and hence, the broadening of the ruby luminescence lines—that is, the e_g and t_{2g} levels in Cr^{3+} (the ruby R lines) should be further split[20]. The change of the crystal structure and distorted octahedra indicate that the electronic and optical properties of the high-pressure phase should be different from that of corundum[20]. The majority of trivalent transition-metal oxides such as Fe_2O_3, Rh_2O_3, Cr_2O_3, Co_2O_3 and Ti_2O_3 crystallize in the corundum structure. High-pressure structural studies of haematite (Fe_2O_3) and rhodium sesquioxide (Rh_2O_3) indicate that these sesquioxides also undergo a phase transformation to the Rh_2O_3 (II)-type structure under pressure[22,29], though the orthorhombic perovskite structure displays a very similar calculated X-ray diffraction pattern.

To understand the effect of the phase transformation on the optical properties of ruby, luminescence spectra were measured under high pressure. No significant difference between the Pt pressure scale[23] and the ruby pressure scale[1,2] was observed below 100 GPa before the phase transformation; however, the luminescence peaks became too weak to be detected in the high-pressure phase (such weakening of the luminescence peaks was also observed in the previous study[4]). Therefore, the laser-heated samples were quenched to ambient conditions for optical measurements. X-ray diffraction showed that the quenched samples had the corundum structure with similar lattice parameters to those of the starting materials. The ruby luminescence

Table 2 Observed and calculated X-ray diffraction peaks of the Rh_2O_3 (II) structure at 113 GPa and 300 K. The unit cell parameters of the Rh_2O_3 (II) structure are a = 6.3900 (±0.0035) Å, b = 4.3624 (±0.0037) Å and c = 4.5452 (±0.0030) Å.

hkl	2θ(deg.)	Obs. d(Å)	Calc. d(Å)	Δd(Å)
200	5.9500	3.1898	3.1950	–0.0053
111	6.7214	2.8240	2.8234	0.0006
002	8.3442	2.2755	2.2726	0.0029
211	8.4619	2.2439	2.2422	0.0018
020	8.7046	2.1815	2.1812	0.0003
102	8.8657	2.1419	2.1412	0.0007
021	9.6662	1.9649	1.9665	–0.0016
310	9.8967	1.9192	1.9140	0.0052
121	10.093	1.8820	1.8795	0.0025
311	10.765	1.7648	1.7640	0.0008
212	11.158	1.7029	1.7047	–0.0018
400	11.908	1.5960	1.5975	–0.0015
022	12.087	1.5724	1.5737	–0.0012
122	12.442	1.5277	1.5280	–0.0003
312	12.971	1.4657	1.4640	0.0017
411	13.357	1.4235	1.4245	–0.0010
113	13.617	1.3964	1.3966	–0.0002

spectra of the quenched Al_2O_3 samples show significant red shifts (Fig. 4). Whereas the R_1 peak of the sample quenched from 90 GPa (the sample was in the corundum structure) occurs at 694.9 nm, the luminescence spectrum of the sample quenched from 136 GPa (the sample was in the Rh_2O_3 (II) and corundum structure) occurs at 696.0 nm (a 'fossilized pressure' of 5.03 GPa according to the ruby pressure scale)[1,2,30]; for comparison, the R_1 peak of ruby normally occurs at 694.2 nm under ambient conditions (Fig. 4). The red shifts and broadening of the ruby luminescence bands are consistent with the different local environments of chromium atoms in the high-pressure structure inferred from diffraction[20]. Shock-wave experiments on corundum have also observed the change of the optical and electrical properties at megabar pressures[7,10–12], consistent with our observations. If corundum were to transform to the orthorhombic perovskite structure under higher pressures as predicted by theoretical calculations[12], the optical and electronic properties should change more significantly because the larger Cr^{3+} cations should prefer larger nine-coordinated sites.

Al_2O_3 is an important oxide component in the Earth's mantle; it is believed that most of the Al_2O_3 stays in the orthorhombic silicate perovskite and that the amount of free Al_2O_3 is probably negligible in the Earth's lower mantle and at the core–mantle boundary. However, the phase transformation and the volume decrease of 3.1% across the phase transition in Al_2O_3 will tend to destabilize this component in silicate perovskite (that is, stabilizing the free Al_2O_3 in the denser form). The transformation may then be important for understanding the physical and chemical properties of the deep lower mantle and D″ zone. Our results on the crystal structure and the elastic properties of this high-pressure phase of Al_2O_3 may therefore give some insight into its role in the Earth's interior, and may help the modelling of Al_2O_3 partitioning between $CaSiO_3$ and $(Mg,Fe)SiO_3$ in the lower mantle.

Received 21 November 2003; accepted 19 March 2004; published online:16 May 2004.

References

1. Mao, H. K., Bell, P. M., Shaner, J. W. & Steinberg, D. J. Specific volume measurements of Cu, Mo, Pd, and Ag and calibration of the ruby R_1 fluorescence pressure gauge from 0.06 to 1 Mbar. *J. Appl. Phys.* **49,** 3276–3283 (1978).
2. Xu, J., Mao, H. K. & Bell, P. M. High pressure ruby and diamond fluorescence: Observations at 0.21 to 0.55 terapascal. *Science* **232,** 1404–1406 (1986).
3. Jephcoat, A. P., Hemley, R. J. & Mao, H. K. X-ray diffraction of Cr^{3+}: Al_2O_3 to 175 GPa. *Physica B* **150,** 115–121 (1988).
4. Funamori, N. & Jeanloz, R. High-pressure transformation of Al_2O_3. *Science* **278,** 1109–1111 (1997).
5. Urtiew, P. A. & Grover, R. Temperature deposition caused by shock interactions with material interfaces. *J. Appl. Phys.* **45,** 140–145 (1974).
6. Grover, R. & Urtiew, P. A. Thermal relaxation at interfaces following shock compression. *J. Appl. Phys.* **45,** 146–152 (1974).
7. Urtiew, P. A. Effect of shock loading on transparency of sapphire crystals. *J. Appl. Phys.* **45,** 3490–3493 (1974).
8. Bass, J., Svendsen, B. & Ahrens, T. J. in *High Pressure Research in Mineral Physics* (eds Manghnani, M. H. & Syono, Y.) 393–402 (Geophys. Monogr. Ser. 39, American Geophysical Union, Washington DC, 1987).
9. Nellis, W. J. & Yoo, C. S. Issues concerning shock temperature measurements of iron and other metals. *J. Geophys. Res.* **95,** 21749–21752 (1990).
10. McQueen, R. G. & Isaak, D. G. Characterizing windows for shock wave radiation studies. *J. Geophys. Res.* **95,** 21753–21765 (1990).
11. Yoo, C. S., Holmes, N. C. & See, E. in *Shock Compression of Condensed Matter* (eds Schmidt, S. C., Dick, R. D., Forbes, J. W. & Tasker, D. G.) 733–736 (Elsevier Science, Amsterdam, 1992).
12. Weir, S. T., Mitchell, A. C. & Nellis, W. J. Electrical resistivity of single-crystal Al_2O_3 shock-compressed in the pressure range 91–220 GPa (0.91–2.2 Mbar). *J. Appl. Phys.* **80,** 1522–1525 (1996).
13. Mashimo, T. *et al.* High-pressure phase transformation of corundum (α-Al_2O_3) observed under shock compression. *Geophys. Res. Lett.* **27,** 2021–2024 (2000).
14. Hama, J. & Suito, K. The evidence for the occurrence of two successive transitions in Al_2O_3 from the analysis of Hugoniot data. *High Temp. High Press.* **34,** 323–334 (2002).
15. Cohen, R. Calculation of elasticity and high pressure instabilities in corundum and stishovite with the potential induced breathing model. *Geophys. Res. Lett.* **14,** 37–40 (1987).
16. Cynn, H., Isaak, D. G., Cohen, R. E., Nicol, M. F. & Anderson, O. L. A high-pressure phase transition of corundum predicted by the potential induced breathing model. *Am. Mineral.* **75,** 439–442 (1990).
17. Marton, F. C. & Cohen, R. E. Prediction of a high-pressure phase in Al_2O_3. *Am. Mineral.* **79,** 789–792 (1994).
18. Thomson, K. T., Wentzcovitch, R. M. & Bukowinski, M. S. T. Polymorphs of alumina predicted by first principles: Putting pressure on the ruby pressure scale. *Science* **274,** 1880–1882 (1996).
19. Duan, W., Wentzcovitch, R. M. & Thomson, K. T. First-principles study of high-pressure alumina polymorphs. *Phys. Rev. B* **57,** 10363–10369 (1998).
20. Duan, W., Paiva, G., Wentzcovitch, R. M. & Fazzio, A. Optical transitions in ruby across the corundum to Rh_2O_3 (II) phase transformation. *Phys. Rev. Lett.* **81,** 3267–3270 (1998).
21. Duan, W., Karki, B. B. & Wentzcovitch, R. M. High-pressure elasticity of alumina studied by first principles. *Am. Mineral.* **84,** 1961–1966 (1999).
22. Shannon, R. D. & Prewitt, C. T. Synthesis and structure of a new high-pressure form of Rh_2O_3. *J. Solid State Chem.* **2,** 134–136 (1970).
23. Holmes, N. C., Moriarty, J. A., Gathers, G. R. & Nellis, W. J. The equation of state of platinum to 660 GPa (6.6 Mbar). *J. Appl. Phys.* **66,** 2962–2967 (1989).
24. Lin, J. F., Shu, J., Mao, H. K., Hemley, R. J. & Shen, G. Amorphous boron gasket in diamond anvil cell research. *Rev. Sci. Instrum.* **74,** 4732–4736 (2003).
25. Shen, G., Rivers, M. L., Wang, Y. & Sutton, S. R. Laser heated diamond cell system at the Advanced Photon Source for in situ X-ray measurements at high pressure and temperature. *Rev. Sci. Instrum.* **72,** 1273–1282 (2001).
26. Watanuki, T., Shimomura, O., Yagi, T., Kondo, T. & Isshiki, M. Construction of laser-heated diamond anvil cell system for in situ x-ray diffraction study at SPring-8. *Rev. Sci. Instrum.* **72,** 1289–1292 (2001).
27. Hammersley, A. P. *FIT2D V10.3 Reference Manual V4.0* (European Synchrotron Radiation Facility, Grenoble, 1998).
28. Larson, A. C. & Von Dreele, R. B. *GSAS Manual* (Report LAUR 86–748, Los Alamos National Laboratory, Los Alamos, 1988).
29. Rozenberg, G. Kh. *et al.* High-pressure structural studies of hematite Fe_2O_3. *Phys. Rev. B* **65,** 064112 (2002).
30. Sobolev, N. V. *et al.* Fossilized high pressure from the Earth's deep interior: The coesite-in-diamond barometer. *Proc. Natl Acad. Sci.* **97,** 11875–11879 (2000).

Acknowledgements

We thank the staff at the BL10XU sector of SPring-8, Japan, and at the HPCAT and GSECARS sectors of the Advanced Photon Source, Argonne National Laboratory, for help with the synchrotron facilities. We also thank G. Shen, V. Prakapenka, M. Yue, O. Yasuo and J. Shu for their assistance in the experiments, and C. Sanloup, R. Hazen, M. Somayazulu, R. Cohen, S. Merkel, Y. Fei and S. Hardy for discussions. This work was supported by the NSF (grant EAR-0217389). Work at Carnegie was supported by DOE/BES, DOE/NNSA (CDAC no. DE-FC03-03NA00144), the NSF and the W.M. Keck Foundation. Correspondence and requests for materials should be addressed to J.-F.L.
Supplementary Information accompanies the paper on www.nature.com/naturematerials

Competing financial interests

The authors declare that they have no competing financial interests.